The Effect of Side Constraint in Rolling Compaction of Powders

Wenhai Wang[1], John C. Cunningham[2], and Antonios Zavaliangos[1]

[1] Drexel University,
Department of Materials Science and Engineering,
Philadelphia, PA 19104
[2] Merck & Co, Inc., West Point, PA 19486

Funding provided by NSF –CMS 0100063

Powder Roll Compaction

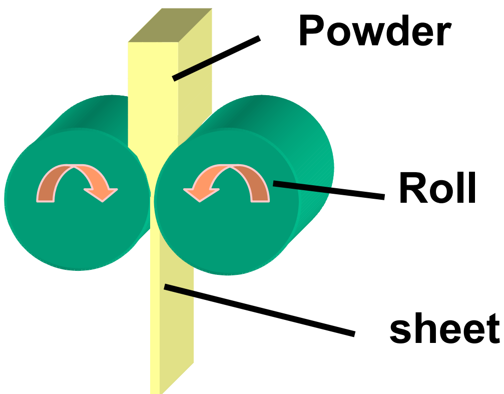

Roll compaction refers the *continuous* compaction of powders by roll mills.

The powder is usually delivered by feed screw to rolls and densified by the *pressure* and *shear force*

Metal:

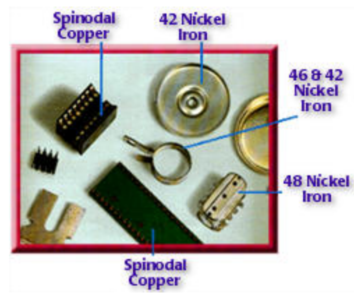

Pharmaceutical:

Chemical:

Food:

Figures copied from http://www.fitzmill.com and http://www.ametekmetals.com

Side Constraints

Roll with side ring

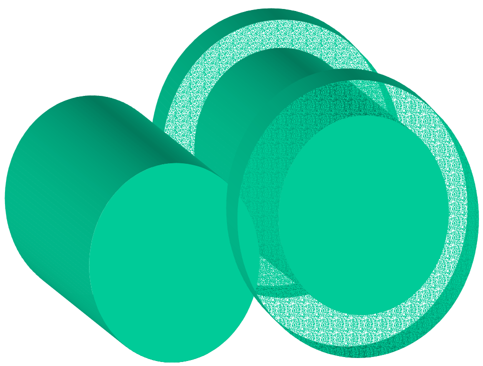

Roll with stationary sidewall

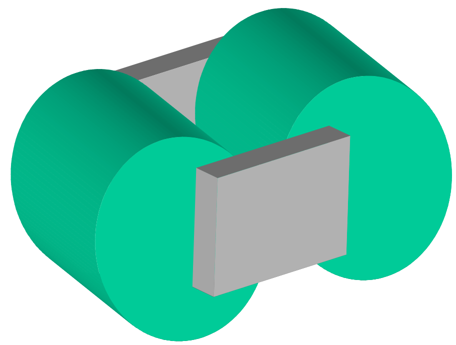

- Side constraints are used to prevent the powder from escaping from the roll gap.
- Friction is unavoidable. (We never roll powder with admixed lubricants)

Experimental Results

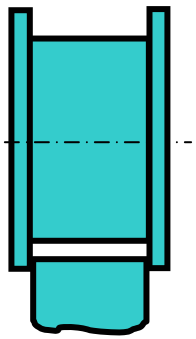

Roll with side ring

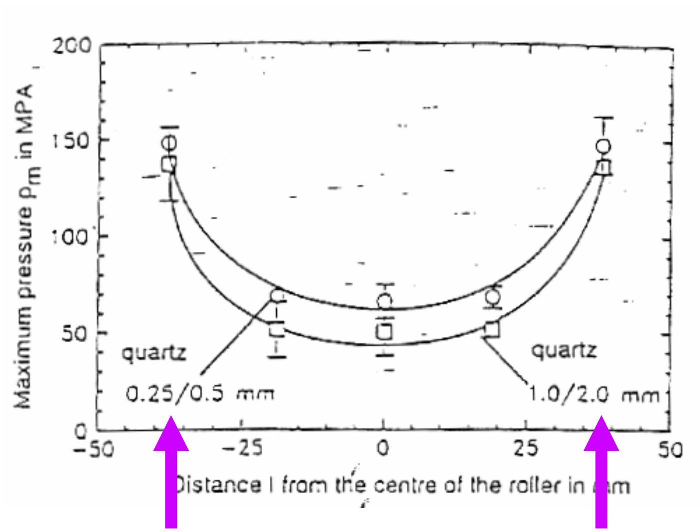

The pressure is highest on the side.

Roll with stationary sidewall

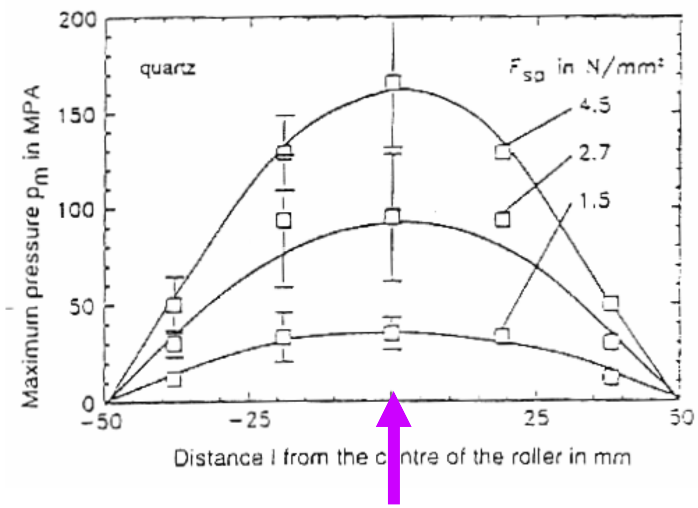

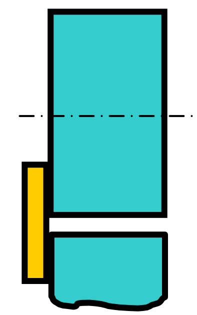

The pressure reaches maximum at center.

U.Lubjuhn, U.Sander, K. Schonert, Zement Kalk Gips, 4/1994, pp. 192-199

Models Development of Roll Compaction

1960, Johanson model Johanson[2] ,Jenike , Shield [3] The first model to predict behavior of the material between the rolls.
1970s-1980s Slab Method V.P. Katashinskii[4,5], M.B.Stern, G.A. Vinogradov, R.T.Dec[6], etc. To predict pressure distribution and roll force in rolling process.
1980s-present Finite Element Model Osakada [7,8], Mori[9], Deshmukh[10], Dec[11], Zavaliangos , Cunningham, etc. FEM simulations on powder compaction.

2. J.R.Johanson, Vol. 32, ser.E, No.4, 1965, pp. 842-848.
3. A.W. Jenike & R.T.Shield, Trans, ASME, vol. 81, 1959, pp. 599-602
4. V.P. Katashinskii & M.B.Stern, Poroshkovaya Metallurgiya, No. 12(252), pp.9-13, 1983
5. V.P . Katashinskii & G.A. Vinogradov, Poroshkovaya Metallurgiya, No. 3(159), pp.31-36, 1976
6. R.T.Dec, Proceedings Inst. Briquetting and Agglomeration, Vol. 22, 1991, pp. 207-218
7. Osakada, Nakano, Mori, Int. J. Mech. Sci., 24-8(1982), 459-468
8. K.Mori, K. Osakada, Int. J. Mech. Sci. 29 (1987), 229
9. A.R. Deshmukh, T.Sundararajan, R.K.Dube, Bhargava, J. of Mate. Proc. Tech. 84(1998) 56-72
10. K.Mori, O.Ebihara, Advanced Tech. of Plast., Vol 2, Proceedings of 6th ICTP, Sept, 19-24,1999
11. Roman T. Dec, Antonios Zavaliangos, John C. Cunningham, Powder Technology 4642, 2002

Objectives

- Explore the nature of density inhomogeneity.
- Evaluate the two kinds of constraint systems using FEM analysis.

Simulated Geometry

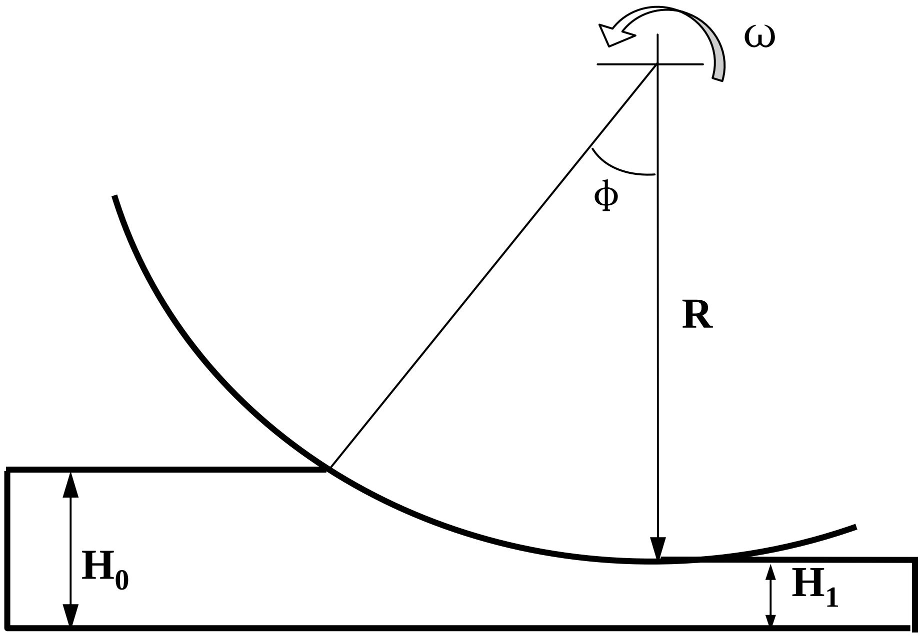

R	=	**200 mm**
$\mathbf{H_0}$	=	**12.06 mm**
$\mathbf{H_1}$	=	**4 mm**
ϕ	=	$\mathbf{20^o}$
ω	=	**0.6 rad**

3D FEM Implementation

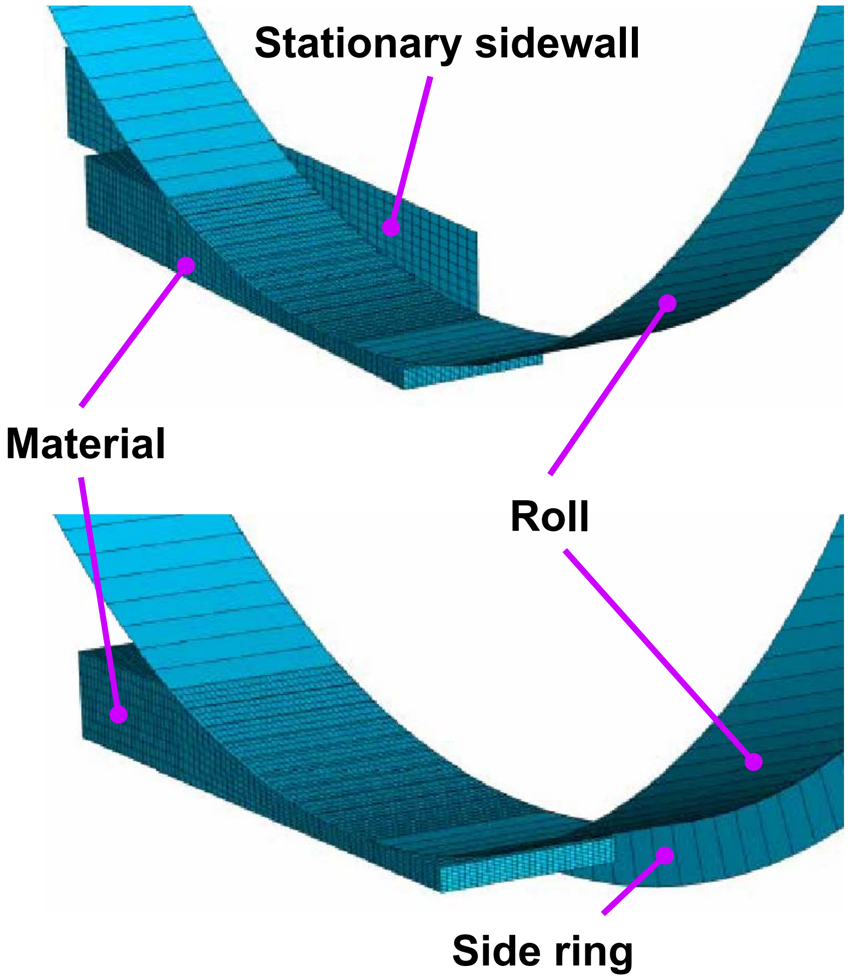

- ABAQUS EXPLICIT;
- One-forth of the geometry due to symmetry (an approximation);
- 16800 3D 8-noded hexahedral elements;
- Roller is modeled with an analytical rigid surface;

3D FEM Implementation (cont.)

- Adaptive remeshing is applied;
- Coulomb friction is assumed upon the contact interfaces;
- Eulerian inflow and outflow boundary condition are implemented at the ends of the rolled specimen;
- Mass scaling is employed to improve computational efficiency;
- Simulation ends when steady state is achieved.

Constitutive models for Porous Materials

Ellipse Model

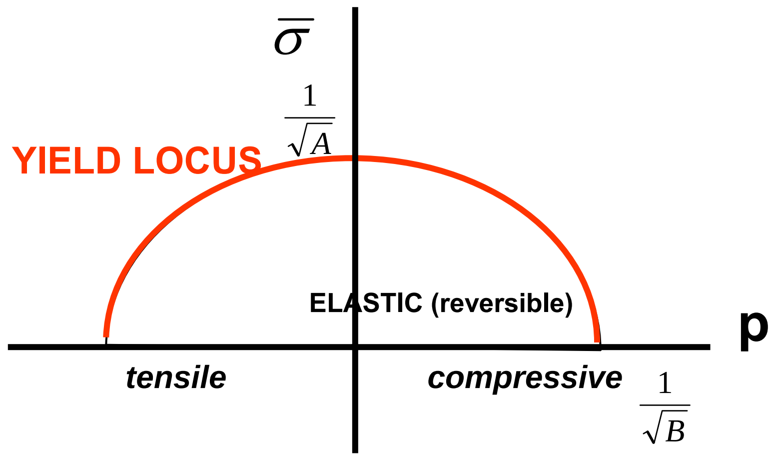

$$\Phi(\overline{\sigma}, p, D) = A(D)\overline{\sigma}^2 + B(D)p^2 - 1 = 0$$

$\overline{\sigma}$ equivalent stress

P hydrostatic pressure

D relative density

Drucker-Prager Model

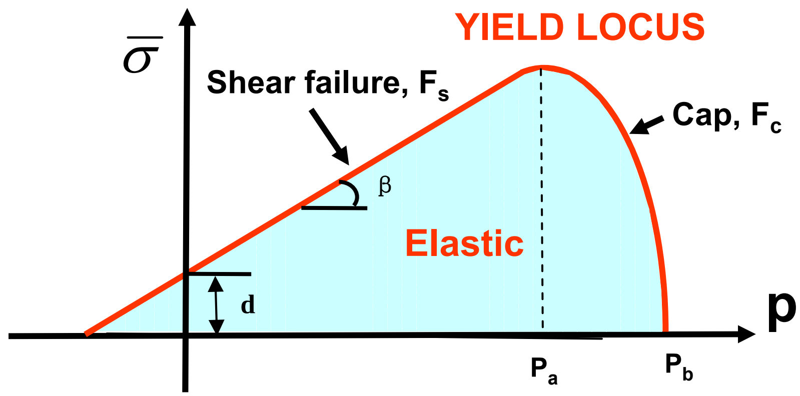

Shear failure region:

$$F_s = \overline{\sigma} - p\tan\beta - d = 0$$

Cap region:

$$F_c = \sqrt{(p - p_a)^2 + (R\overline{\sigma})^2} + R(d + p_a\tan\beta) = 0$$

- **D-P model is more appropriate but numerical implementation in ABAQUS has problems;**
- **Gurson's model is chosen (overestimates loads).**

Gurson's Model

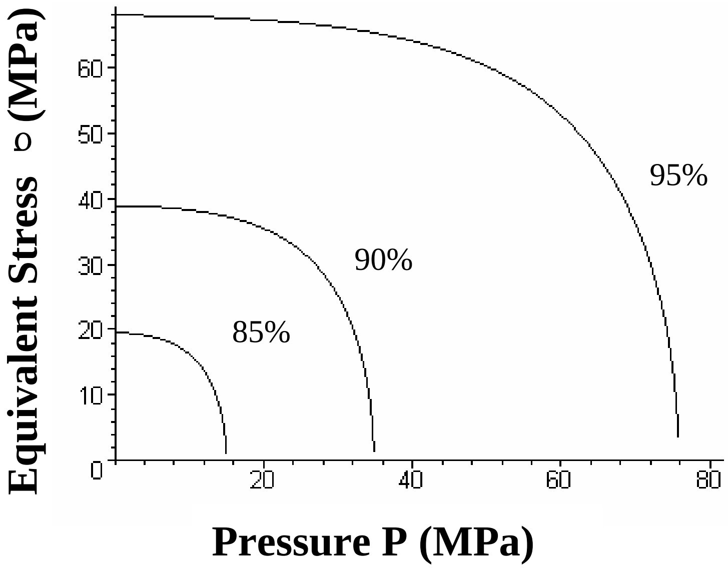

where $\overline{\sigma}$ is the effective Mises stress: $\overline{\sigma} = \sqrt{\frac{3}{2} S \bullet S}$;

S is the deviatoric part of the cauchy stress tensor ;

P is the hydrostatic pressure

f is the porosity of the material.

$$\Phi(\overline{\sigma}, P, f) = \left(\frac{\overline{\sigma}}{\sigma_Y}\right)^2 + 2q_1 f \cosh\left(-q_2 \frac{3P}{2\sigma_Y}\right) - (1 + q_3 f^2) = 0$$

Cases Studied

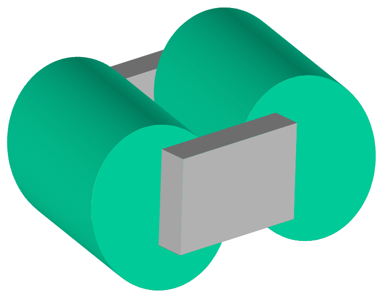

Stationary sidewall with $\mu = 0.4$ **at powder/wall and powder/roll interface;**

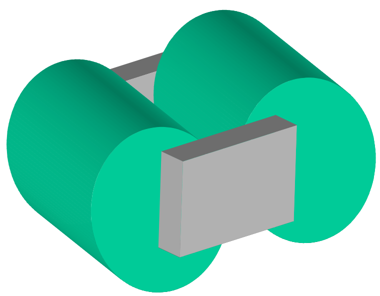

Stationary sidewall with $\mu = 0$ **at powder/wall and** $\mu = 0.4$ **at powder/roll interface;**

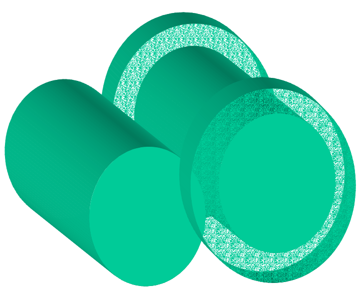

Roll with side ring, with $\mu = 0.4$ **everywhere.**

Pressure Distribution Along Roll Direction

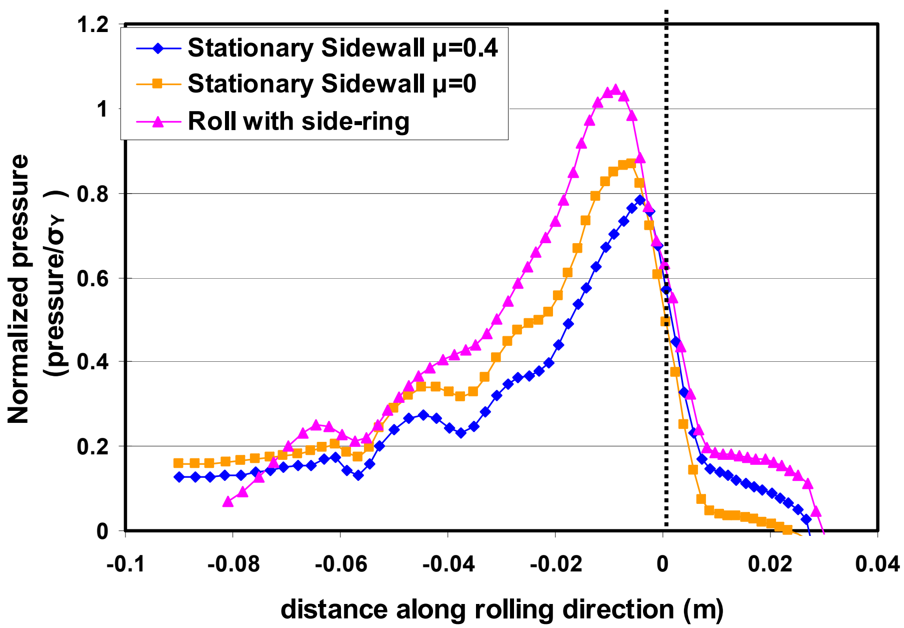

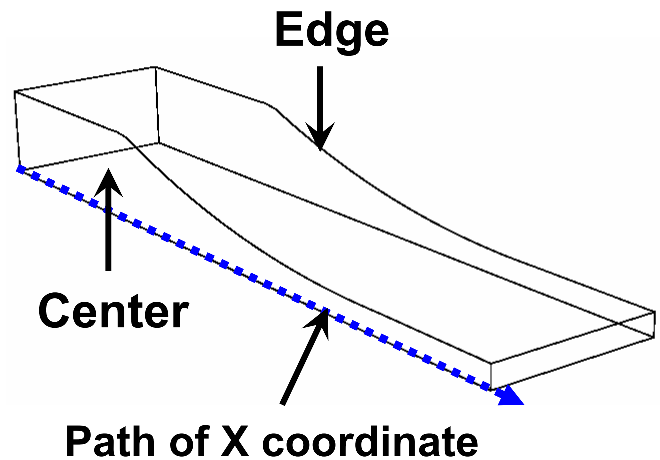

Roll pressure rises to a maximum just before the exit.

Pressure Distribution along Roll Width

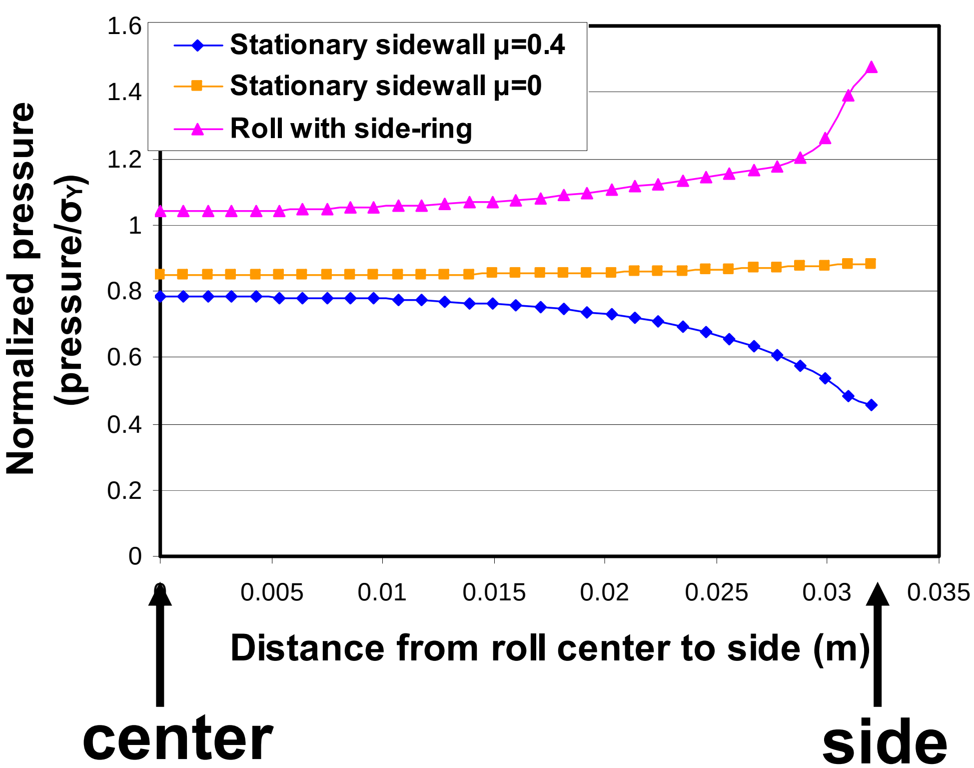

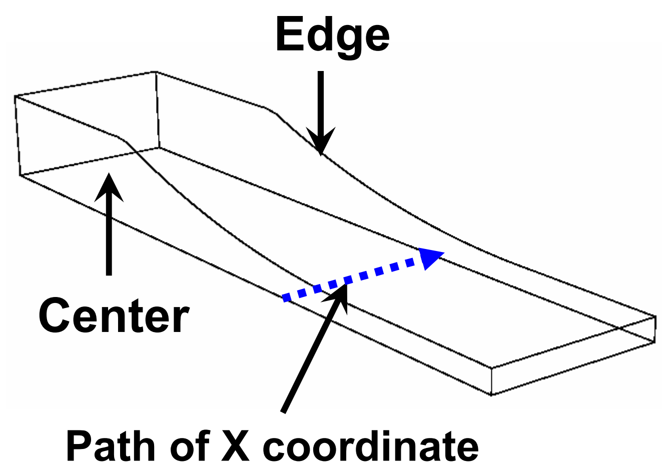

Inhomogeneous **pressure distribution along roll width for all cases with** $\mu \neq 0$ **.**

Porosity Evolution

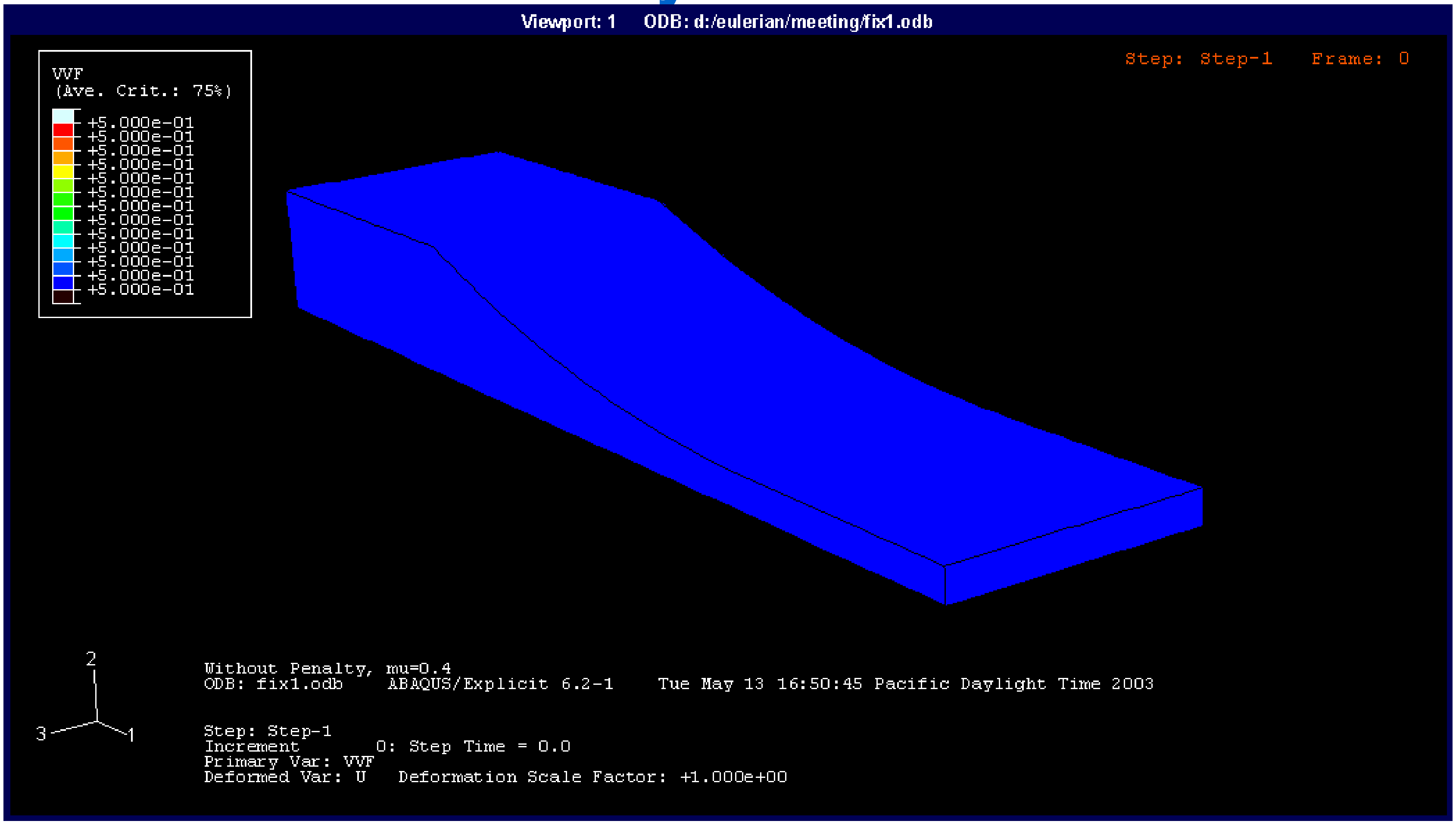

Stationary sidewall with $\mu = 0.4$ at powder/wall and powder/roll interface.

Porosity Distribution along Roll Width

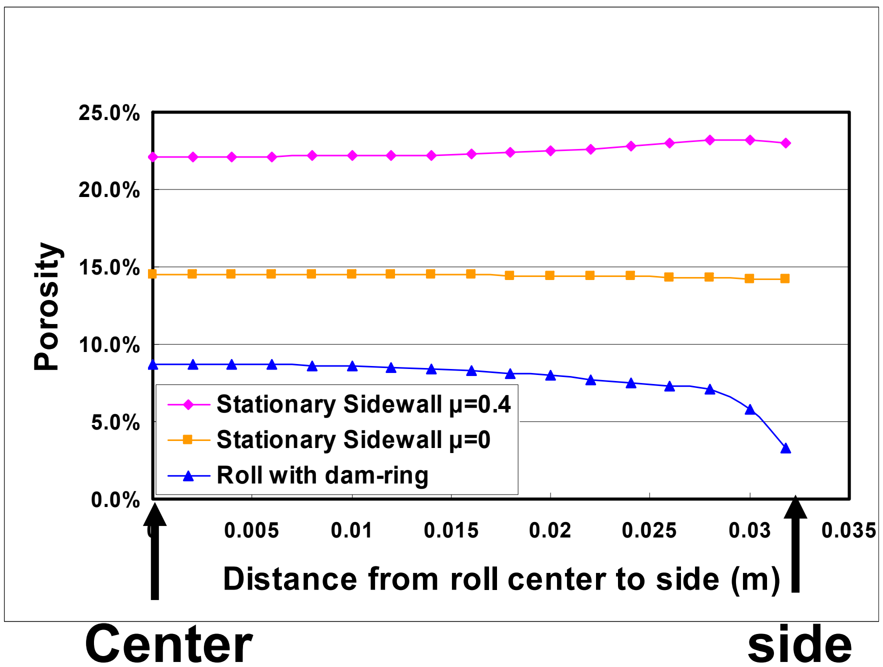

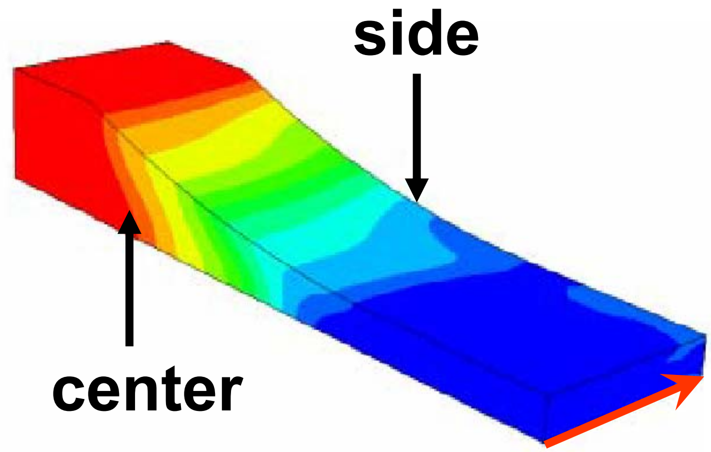

Porosity roll with "dam-ring" < **Porosity** roll with "stationary sidewall"

Entrance Velocity

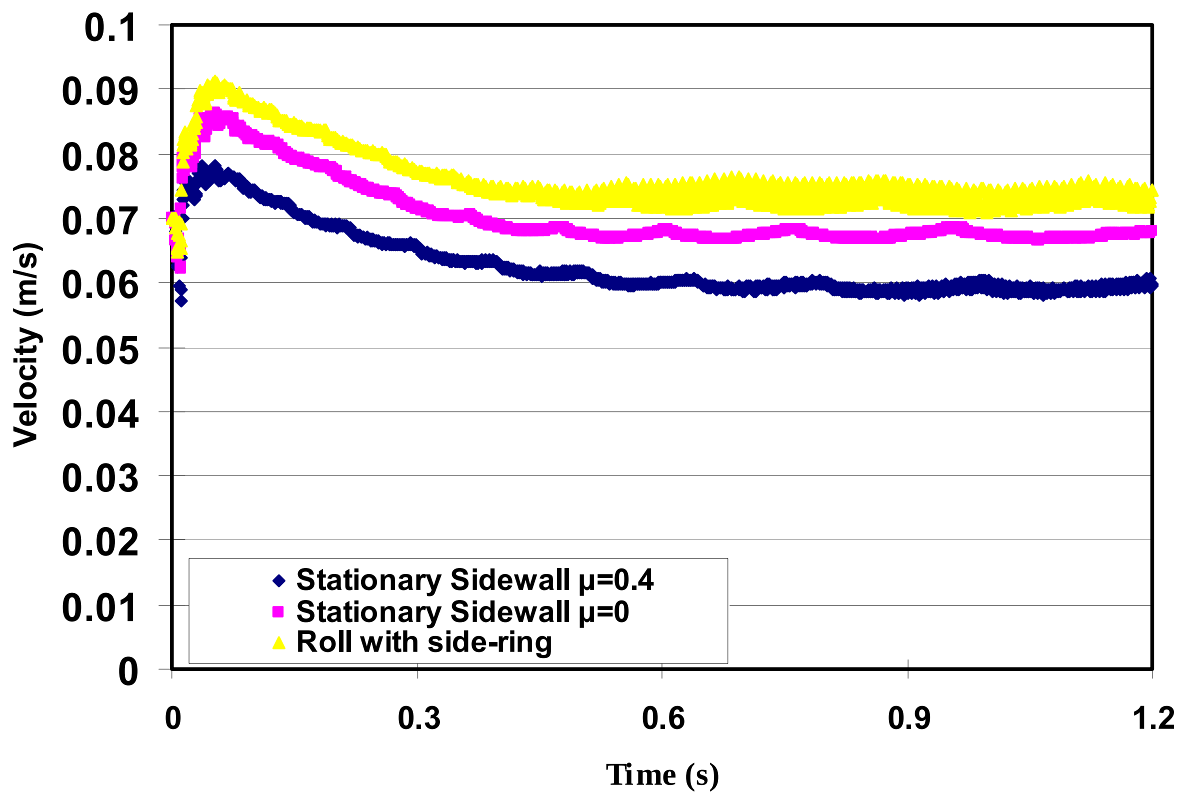

At the same ω, roll with side ring has higher throughout.

Roll Force Evolution

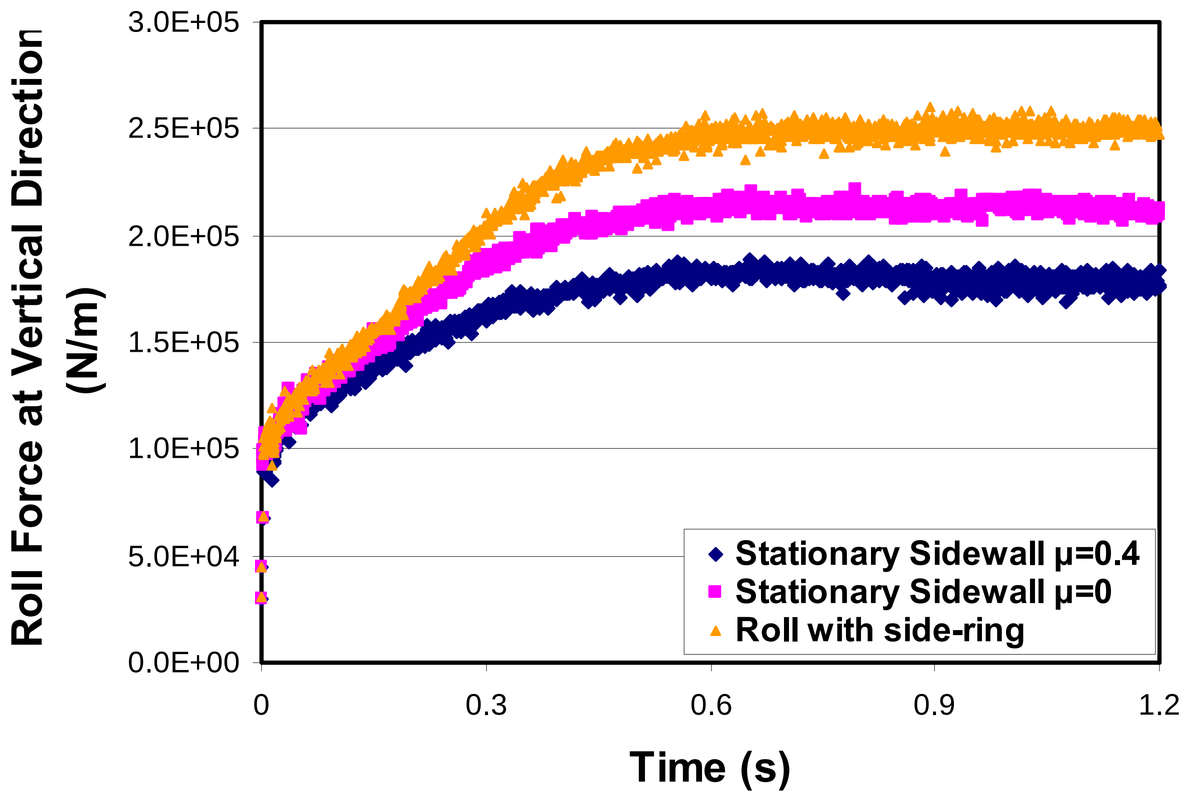

RF_2 higher for side ring because the achieved density is much higher.

Conclusions

- Simulation results replicates experimental trends in pressure distribution.
- Inhomogeneity has its origin in the friction with constraints.
- Side ring results a much more efficient densification, but it does not eliminate porosity variation.
- Minimization of the property variation requires elimination of the frictional interaction between powder and side constraint.

Future Work

1. More realistic constitutive models for both material and friction are needed.

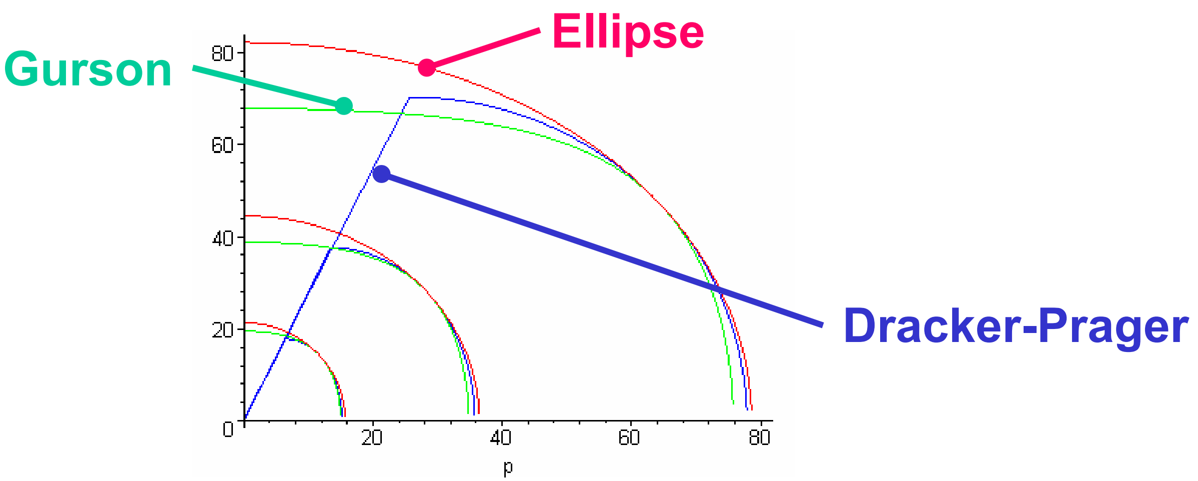

2. Further verification with experiments.